Biochemical Pharmacology 87 (2014) 229–242

Contents lists available at ScienceDirect

Biochemical Pharmacology

journal homepage: www.elsevier.com/locate/biochempharm

Andrographolide downregulates the v-Src and Bcr-Abl oncoproteins and induces Hsp90 cleavage in the ROS-dependent suppression of cancer malignancy

Sheng-Hung Liu [a,b], Chao-Hsiung Lin [b,c], Fong-Ping Liang [d], Pei-Fen Chen [d], Cheng-Deng Kuo [e], Mohd. Mujahid Alam [f], Barnali Maiti [f], Shih-Kai Hung [g], Chin-Wen Chi [a,b], Chung-Ming Sun [f,**], Shu-Ling Fu [b,d,*]

[a] Department and Institute of Pharmacology, National Yang-Ming University, Taipei 11221, Taiwan
[b] Program in Molecular Medicine, National Yang-Ming University and Academia Sinica, Taipei 11221, Taiwan
[c] Department of Life Sciences and Institute of Genome Sciences, National Yang-Ming University, Taipei 11221, Taiwan
[d] Institute of Traditional Medicine, National Yang-Ming University, Taipei 11221, Taiwan
[e] Department of Research and Education, Taipei Veterans General Hospital, Taipei 11217, Taiwan
[f] Department of Applied Chemistry, National Chiao Tung University, Hsinchu 30013, Taiwan
[g] Department of Radiation Oncology, Buddhist Dalin Tzu Chi General Hospital, Chiayi, Taiwan

ARTICLE INFO

Article history:
Received 10 August 2013
Accepted 15 October 2013
Available online 24 October 2013

Keywords:
Andrographolide
Hsp90
Src
Bcr-Abl
ROS
Apoptosis

ABSTRACT

Andrographolide is a diterpenoid compound isolated from *Andrographis paniculata* that exhibits anticancer activity. We previously reported that andrographolide suppressed v-Src-mediated cellular transformation by promoting the degradation of Src. In the present study, we demonstrated the involvement of Hsp90 in the andrographolide-mediated inhibition of Src oncogenic activity. Using a proteomics approach, a cleavage fragment of Hsp90α was identified in andrographolide-treated cells. The concentration- and time-dependent induction of Hsp90 cleavage that accompanied the reduction in Src was validated in RK3E cells transformed with either v-Src or a human truncated c-Src variant and treated with andrographolide. In cancer cells, the induction of Hsp90 cleavage by andrographolide and its structural derivatives correlated well with decreased Src levels, the suppression of transformation, and the induction of apoptosis. Moreover, the andrographolide-induced Hsp90 cleavage, Src degradation, inhibition of transformation, and induction of apoptosis were abolished by a ROS inhibitor, N-acetyl-cysteine. Notably, Hsp90 cleavage, decreased levels of Bcr-Abl (another known Hsp90 client protein), and the induction of apoptosis were also observed in human K562 leukemia cells treated with andrographolide or its active derivatives. Together, we demonstrated a novel mechanism by which andrographolide suppressed cancer malignancy that involved inhibiting Hsp90 function and reducing the levels of Hsp90 client proteins. Our results broaden the molecular basis of andrographolide-mediated anticancer activity.

1. Introduction

Heat shock protein 90 (Hsp90) is an ATP-dependent molecular chaperone that is required for the folding, activation, maturation and stability of client proteins. Many Hsp90 client proteins participate in essential cell physiology [1]. Previously, it was reported that solid tumors and hematological cancers had a higher expression of Hsp90 and its co-chaperones than normal cells [2–4]. In addition, many proteins known to promote carcinogenesis, including oncoproteins (such as v-Src and Bcr-Abl) and signal-transducing proteins (such as Akt and HER2), are Hsp90 client proteins. Furthermore, Hsp90-mediated stabilization/activation of these client proteins contributes to the acquisition of cancer cell hallmarks, including proliferation, survival, angiogenesis and invasion [5,6].

Cancer cells are more susceptible to Hsp90 inhibition than normal cells [7]. Upon Hsp90 inhibition, cancer-associated client proteins cannot adopt their active conformations and therefore get degraded, losing the ability to maintain pathways that are essential for the malignant phenotypes of cancer cells. For example, the Akt pathway is involved in the survival and metastasis of cancer cells

* Corresponding author at: Institute of Traditional Medicine, National Yang-Ming University, Taipei 11221, Taiwan. Tel.: +886 2 28267177; fax: +886 2 28225044.
** Corresponding author. Tel.: +886 3 5131511; fax: +886 3 5736007.
E-mail addresses: cmsun@mail.nctu.edu.tw (C.-M. Sun), slfu@ym.edu.tw (S.-L. Fu).

0006-2952/$ – see front matter © 2013 Elsevier Inc. All rights reserved.
http://dx.doi.org/10.1016/j.bcp.2013.10.014

[8], and inhibiting Hsp90 disrupts the association of Akt with the Hsp90-Cdc37 complex, leading to proteasome-dependent Akt degradation [9]. Bcr-Abl, the oncoprotein responsible for chronic myelogenous leukemia (CML), is a molecular target for clinical CML treatment [10]. Hsp90 inhibition promotes Bcr-Abl degradation and suppresses the proliferation of Bcr-Abl-expressing CML [11,12]. In addition, Hsp90 as well as its co-chaperones are essential for the maturation and stability of the v-Src oncoprotein and therefore for sustaining v-Src-mediated cellular transformation [13–15]. Because Hsp90 inhibition abolishes the client-mediated pathways that are essential for cancer malignancy and leads to cancer cell death, Hsp90 inhibitors are considered promising agents for cancer chemotherapy [16].

In vertebrates, inducible Hsp90α and constitutively expressed Hsp90β are the two major isoforms of Hsp90. The Hsp90 protein contains three major domains with specific functions. The N-terminal domain consists of an adenine nucleotide-binding pocket that is involved in ATP binding and hydrolysis. The middle domain is responsible for regulating ATP hydrolysis and the interactions with client proteins and co-chaperones. The C-terminal domain contains a conserved MEEVD motif that plays a role in the recruitment of TPR-domain-containing co-chaperones. Hsp90 acts as a homodimer of two Hsp90 molecules that associate via the C-terminal domain [1,17]. Most Hsp90 inhibitors, such as geldanamycin, 17-AAG and radicicol, bind to the N-terminal ATP-binding pocket to suppress Hsp90 activity [18]. Several coumarin derivatives interact with the C-terminus of Hsp90, providing an alternative targeting strategy for Hsp90 inhibitors [16]. Recently, it was reported that the chaperone activity of Hsp90 proteins could be attenuated by oxidative stress-induced Hsp90 cleavages. Various Hsp90α and Hsp90β cleavage products have been identified in cancer cells under oxidative stress caused by treatments such as ascorbate/menadione [19], H_2O_2 [20,21] and arsenate [22]. Hsp90 cleavage is accompanied by the reduced expression of client proteins and the induction of cancer cell apoptosis [19,22]. Therefore, Hsp90 cleavage may represent another mechanism to inhibit Hsp90 function.

Andrographolide (Fig. 1), a diterpenoid lactone isolated from *Andrographis paniculata*, is the major constituent of *A. paniculata.* Andrographolide has been reported to exhibit anti-inflammatory activities *in vitro* and *in vivo*. Andrographolide suppresses the secretion of cytokines, chemokines and inflammatory enzymes (iNOS and COX) from macrophages [23–25]. In a murine asthma model, andrographolide suppressed allergic lung inflammation by inhibiting the NF-κB pathway [23,26]. Recently, accumulating evidence indicates that andrographolide potently inhibits numerous malignant cancer phenotypes [27–30]. Andrographolide inhibited cell cycle progression in human colorectal carcinoma and hepatoma cells [27,28]. Furthermore, andrographolide induced the apoptosis of human hepatoma HepG2 cells via the caspase 8-dependent activation of pro-apoptotic Bcl-2 family members [29] and sensitized cancer cells to TRAIL-induced apoptosis in a p53-dependent manner [30]. Andrographolide also promoted autophagic cell death and increased ROS in human liver

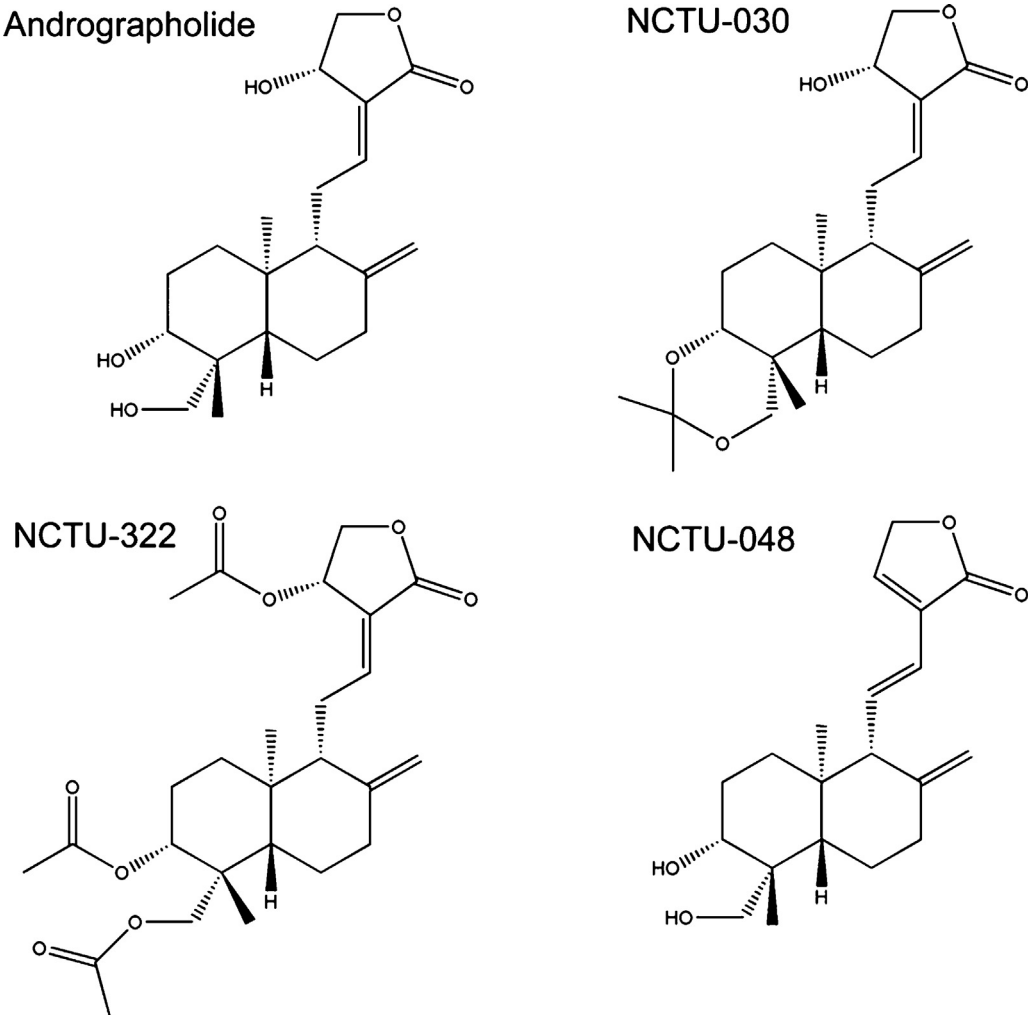

Fig. 1. Chemical structures of andrographolide and its derivatives.

cancer cells [31]. Moreover, andrographolide increased the radiosensitivity and chemosensitivity of cancer cells [32,33]. Several reports have demonstrated that andrographolide suppresses cancer invasion by inhibiting the activity of matrix metalloproteinases (MMPs) [34,35]. Our previous work has demonstrated that andrographolide suppresses v-Src-induced cellular transformation by promoting v-Src degradation [36]. In this study, we further investigated the molecular mechanism of andrographolide-induced v-Src degradation. Using a proteomic strategy, we identified an Hsp90 fragment that was induced by andrographolide treatment. Furthermore, we demonstrated that andrographolide-induced Hsp90 cleavage was ROS-dependent and that the induction of Hsp90 cleavage by andrographolide was associated with the downregulation of Hsp90 client proteins and the suppression of cancer cell malignancy.

2. Materials and methods

2.1. Chemicals and antibodies

Andrographolide and N-acetylcysteine (NAC) were purchased from Sigma-Aldrich (St. Louis, MO). Andrographolide derivatives (NCTU-030, NCTU-048 and NCTU-322) were synthesized by Dr. Chung-Ming Sun at the Department of Applied Chemistry, National Chiao Tung University, Hsinchu, Taiwan. Antibodies against v-Src (clone EC10) and Src were purchased from Upstate Biotechnology (Lake Placid, NY). Anti-Hsp90 antibodies against different regions of Hsp90 (Cat No. 4874 and 4877) and the anti-Bcr antibody were purchased from Cell Signaling Technology (Beverly, CA). Anti-Hsp90α and anti-GAPDH antibodies were purchased from GeneTex (Irvine, CA). The anti-actin antibody was purchased from Sigma-Aldrich (St. Louis, MO).

2.2. Cell culture

RK3E/ts-v-Src, v-Src#1 and Src531#6 cells were created and cultured as previously described [36]. Src531 is a C-terminally truncated Src mutant previously identified in human colon cancer cells [37]. K562 cells were regularly maintained in RPMI medium (Gibco, Grand Island, NY) containing 10% fetal bovine serum (Biological Industries, Kibbutz Beit Haemek, Israel), 1% penicillin-streptomycin-glutamine, and 1% sodium pyruvate (Gibco, Grand Island, NY) in a 5% CO_2 humidified incubator at 35 °C.

2.3. Determination of morphological alterations

The ts-v-Src cells (10^5) were seeded in MP-6 plates and grown at 39.5 °C overnight. The cells were treated with vehicle or drugs and immediately incubated at 35 °C. After 24 h, cell morphology was photographed under a phase-contrast microscope at 200× magnification.

2.4. Western blot

Vehicle- and drug-treated cells were collected and lysed in RIPA buffer [50 mM Tris (pH 7.4), 150 mM NaCl, 1% Nonidet P-40, 0.25% sodium deoxycholate, 5 mM EDTA (pH 8.0), and 1 mM EGTA (pH 8.0)] containing 0.5% protease inhibitor cocktail (Sigma-Aldrich, St. Louis, MO). Total protein (50 μg) was analyzed as described previously [38].

2.5. IEF and 2-DE

The ts-v-Src cells (3×10^5/100 mm dish) were treated with 0.1% DMSO, andrographolide (10 μM) or NCTU-048 (10 μM) for 4 h at 35 °C. The cells were harvested and lysed in 25 mM Tris–Cl buffer (pH 8.0) containing protease inhibitors (Sigma-Aldrich, St. Louis, MO). Sample preparation and analysis were performed as described previously [39]. For the 2-DE analysis, 500 μg of total protein was precipitated with methanol/chloroform. The protein pellets were dissolved in 250 μl of rehydration buffer [7 M urea, 2 M thiourea, 4% CHAPS, 2% IPG buffer (Amersham Bioscience, Piscataway, NJ), 1.2% DeStreak reagent (Amersham Bioscience) and 0.002% bromophenol blue (Amersham Bioscience)]. For rehydration, the samples were loaded into 13 cm Immobiline DryStrips (Amersham Bioscience) with a 3–10 pH gradient for 12 h. 2-DE was performed according to the supplier's protocol (Amersham Bioscience).

2.6. LC–MS/MS analysis

To identify the proteins, trypsin-digested peptides were dried and dissolved in H_2O (0.1% formic acid) for LTQ-Orbitrap hybrid tandem mass spectrometry (Thermo Fisher Scientific, Bremen, Germany). The parameters for the LC–MS/MS and mass spectrometry analyses were described previously [40].

2.7. Annexin V/PI staining

The ts-v-Src cells (3×10^5) were seeded in 100-mm plates, grown overnight at 35 °C and treated with vehicle, andrographolide or an andrographolide derivative for 24 h. The apoptotic cells were detected using an Annexin V-fluorescein isothiocyanate-conjugated kit (R&D, Minneapolis, MN) and flow cytometry (FACSCalibur, Becton Dickinson, San Jose, CA). The Annexin V^+ cells were calculated as apoptotic cells.

2.8. ROS measurements

ROS levels were measured using dichlorofluorescein diacetate (H_2DCFDA, Invitrogen, Grand Island, NY). Drug-treated cells were incubated with 10 μM H_2DCFDA in PBS at 37 °C for 30 min, and the dye-labeled cells were incubated in growth medium (DMEM, 10% FBS, 1% P.S.G. and 1% sodium pyruvate) at 37 °C for 1 h. Subsequently, the cells were washed and resuspended in PBS and stained with PI (10 μg/ml). The intensity of the green fluorescence in PI-negative cells was determined by flow cytometry. Superoxide levels were measured using MitoSOX (Invitrogen, Grand Island, NY). Briefly, the drug-treated cells were incubated with 5 μM MitoSOX in HBSS at 37 °C for 15 min. Subsequently, these cells were washed twice and resuspended in HBSS. The intensity of red fluorescence in treated cells was determined by flow cytometry.

2.9. Measurement of the intracellular level of glutathione

Levels of intracellular glutathione were measured using glutathione assay kit (Sigma-Aldrich, St. Louis, MO) and calculated for quantitative analysis. Briefly, the drug-treated cells (10^6 cells) were resuspended in 5-sulfosalicylic acid (5%), frozen-and thaw twice, then left at 4°C for 5 min. After centrifugation at 10,000 × g for 10 min, the supernatant was collected and measured for the glutathione levels following manufacturer's instruction. The GSH level was shown as nmole per 10^6 cells.

2.10. Statistics

The data are expressed as the mean ± SD of three independent experiments. A p-value of <0.05 indicated a statistically significant difference as determined by Student's t-test.

3. Results

3.1. The effects of andrographolide derivatives on v-Src expression and transformation

We previously demonstrated that andrographolide suppressed v-Src-induced transformation by decreasing the stability of v-Src [36]. To further investigate the inhibitory effects of andrographolide derivatives (Fig. 1), a sublethal concentration of each compound based on MTT assay data (data not shown) was chosen to determine the inhibition of v-Src-induced transformation using a temperature-sensitive v-Src-expressing cell line (ts-v-Src). ts-v-Src cells grown at 39.5 °C were treated with andrographolide or its derivatives, immediately switched to a 35 °C incubator and cultured for another 24 h. Andrographolide (Andro), NCTU-030 and NCTU-322 significantly suppressed v-Src-induced cell transformation (Fig. 2A). In contrast to the transformed ts-v-Src cells grown at 35 °C that displayed more membrane extensions and lost their cell-cell contacts, the cells treated with these compounds exhibited flat polygonal morphology with clear cell-cell contacts, similar to the non-transformed morphology observed in ts-v-Src cells grown at 39.5 °C. Conversely, NCTU-048 did not affect v-Src-mediated morphological transformation (Fig. 2A). We next investigated whether andrographolide derivatives also affected v-Src protein expression. As shown in Fig. 2B, NCTU-030 and NCTU-322, but not NCTU-048, significantly reduced v-Src expression. Accordingly, the ability of andrographolide derivatives to suppress transformation correlated with the ability to attenuate v-Src expression.

3.2. Identification of an Hsp90α fragment in andrographolide-treated cells

To further investigate the mechanism of andrographolide-mediated inhibition of cellular cell transformation and v-Src degradation, we compared the proteomes of ts-v-Src cells treated with vehicle control, andrographolide or NCTU-048. NCTU-048 was included as a reference control because it has a similar structure to andrographolide but did not exhibit any inhibitory effects. We specifically identified proteins that exhibited altered expression in andrographolide-treated cells but not in the other cells. Presumably, these proteins were more relevant to andrographolide-mediated transformation inhibition and v-Src degradation. Overall, 11 up-regulated spots and 5 downregulated spots were selected from the gel images of andrographolide-treated cells and subsequently analyzed by LC–MS/MS. Among these, an Hsp90α fragment was identified; the peptide sequence was deduced from the MS spectra and was mapped to the N-terminus of Hsp90α (Fig. 3A and B). We next verified the proteomics data by Western blot using antibodies against Hsp90α and Hsp90α/β. A cleaved Hsp90 fragment was detected in transformed ts-v-Src cells treated with andrographolide (10 μM), which is in accordance with the proteomic data (Fig. 3C).

3.3. Andrographolide treatment in various Src-transformed cells induced Hsp90 cleavage in a concentration- and time-dependent manner

Since Hsp90 has been reported to regulate the stability of v-Src and v-Src-induced cell transformation [1,41], we next determined whether Hsp90 cleavage was a key event in the andrographolide-mediated decrease in v-Src and the resulting biological effects. As described in our previous study, andrographolide treatment of ts-v-Src cells under different conditions could lead to Src down-regulation but caused different biological consequences [36]. When ts-v-Src cells grown at 39.5 °C (non-transformed phenotype) were treated with andrographolide and immediately incubated at 35 °C for 24 h, transformation was inhibited. However, when ts-v-Src cells constantly grown at 35 °C (transformed phenotype) were treated with andrographolide at 35 °C for 24 h, they underwent significant cell death. We next investigated whether andrographolide caused Hsp90 cleavage in ts-v-Src cells under both conditions. When ts-v-Src cells grown at 35 or 39.5 °C were treated with andrographolide and then cultured at 35 °C for 24 h, Hsp90 cleavage occurred in a dose-dependent manner under both conditions (Fig. 4A). Moreover, the andrographolide-mediated downregulation of v-Src correlated with the production of the Hsp90 fragment in both conditions (Fig. 4A). The induction of Hsp90 cleavage was also measured in andrographolide-treated transformed cells constitutively expressing wild-type v-*src* (v-Src#1 cells) or the truncated mutant of human c-*src* (Src531 cells). As shown in Fig. 4B, andrographolide treatment induced Hsp90 cleavage in both cell types. Furthermore, andrographolide treatment also reduced Src protein expression in these cells. In a time-course experiment, Hsp90 cleavage in v-Src-overexpressing cells was induced after 6 h of andrographolide treatment, and the maximal expression of the Hsp90 fragment occurred at 24 h (Fig. 4C).

3.4. Hsp90 cleavage correlated with andrographolide-induced apoptosis

We previously demonstrated that andrographolide treatment of v-Src transformed cells induced significant cell death and that most of the dead cells were detached [36]. The induced expression of cleaved Hsp90 in adherent and detached v-Src-transformed cells after andrographolide treatment was investigated. As shown in Fig. 5A, a higher level of cleaved Hsp90 was detected in detached cells than in adherent cells. In addition, the expression of v-Src in these cells was inversely correlated with the amount of cleaved Hsp90. To determine whether andrographolide-mediated cell death involved apoptosis, Annexin V/PI staining was performed in cells treated with different concentrations of andrographolide. Apoptotic cells were evident after treatment with 10 μM andrographolide (Fig. 5B), and the degree of apoptosis was more significant in detached cells (Fig. 5C). Together, these data demonstrated that andrographolide-mediated Hsp90 cleavage was associated with decreased v-Src as well as with apoptosis.

3.5. Apoptosis induction by andrographolide derivatives correlated with the ability to induce Hsp90 cleavage

For several andrographolide derivatives, the ability to inhibit transformation correlated with the reduction in Src expression (Fig. 2). We further investigated whether Hsp90 cleavage was associated with v-Src degradation and apoptosis induced by andrographolide derivatives. Transformed ts-v-Src cells treated with andrographolide derivatives (NCTU-030 and NCTU-322) exhibited a dramatic increase in Hsp90 cleavage, similar to that observed with andrographolide (Fig. 6A). However, NCTU-048 treatment did not increase v-Src degradation or Hsp90 cleavage. Only the active derivatives of andrographolide (NCTU-030 and NCTU-322) induced apoptosis in transformed ts-v-Src cells (Fig. 6B). These results confirmed the strong correlation between andrographolide-induced Hsp90 cleavage and the inhibition of v-Src-mediated oncogenicity.

3.6. ROS production was involved in andrographolide-mediated Hsp90 cleavage

Oxidative stress-induced Hsp90 cleavage has been described previously [19,42]. Moreover, andrographolide treatment has been

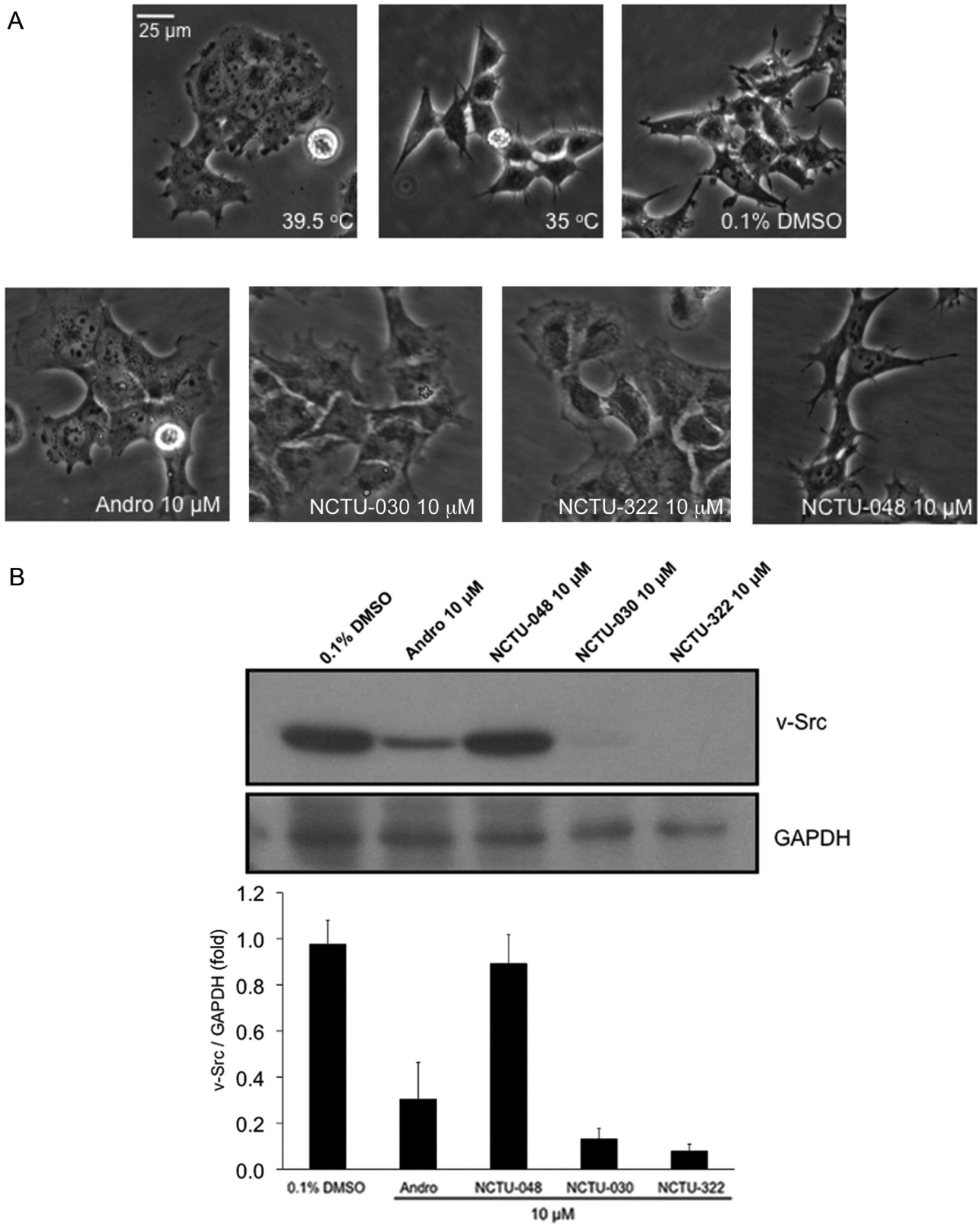

Fig. 2. Inhibition of v-Src transformation by andrographolide and its derivatives. (A) The effects of andrographolide and its derivatives on v-Src-induced cell transformation were evaluated. The ts-v-Src cells were treated with vehicle (0.1% DMSO) or various drugs at the indicated concentrations, switched from 39.5 to 35 °C, grown for 24 h, and observed by microscopy for morphological alterations. ts-v-Src cells grown at 39.5 or 35 °C served as controls for the non-transformed and transformed phenotypes, respectively. (B) Western blotting was utilized to analyze the v-Src levels in drug-treated cells 24 h after switching to 35 °C. GAPDH served as the internal control.

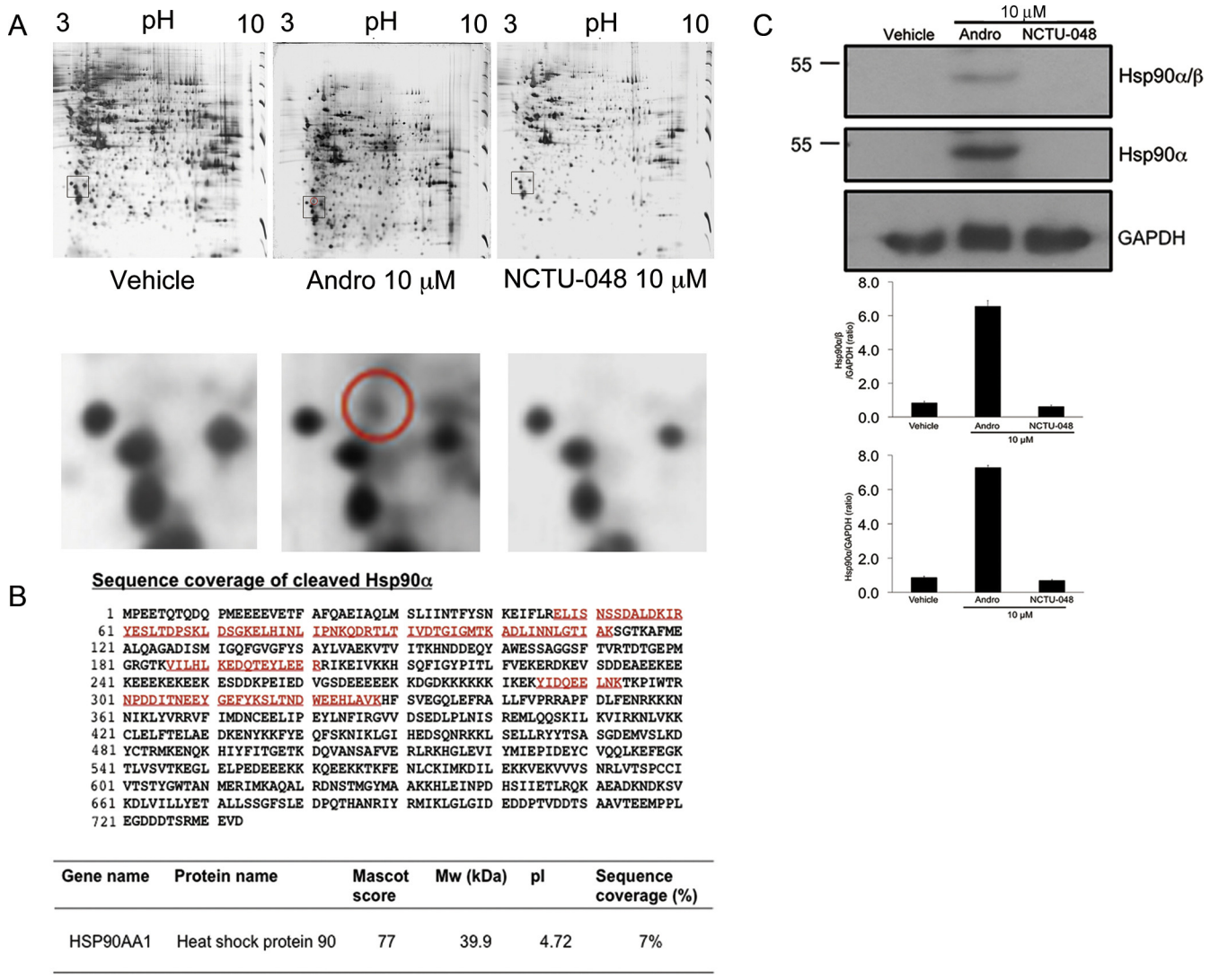

Fig. 3. An Hsp90α fragment was identified in andrographolide-treated cells. (A) A total of 500 μg of protein lysate from the vehicle-, andrographolide- and NCTU-048-treated ts-v-Src cells was subjected to 2-DE analysis. The resulting 13 cm × 13 cm, pH 3-10 2D gels were stained with silver nitrate and analyzed by imaging software to identify the differentially expressed proteins in response to drug treatment. The circled spot in the enlarged area was more intense in the andrographolide-treated group compared with the others and was further analyzed by MS to determine its identity. (B) The peptide sequences (underlined) identified from the MS spectra mapped to the N-terminal region of Hsp90α (*top panel*). The characteristics of the identified Hsp90α fragment are listed in the bottom panel. (C) The increased expression of the Hsp90α fragment after andrographolide treatment (10 μM, temperature switch, 24 h) was verified by Western blot. Antibodies against Hsp90α/β and Hsp90α were utilized to detect the presence of the Hsp90 fragment.

reported to involve ROS induction in cancer cells [28,43]. We therefore investigated whether andrographolide induced Hsp90 cleavage via ROS. The ROS levels in andrographolide-treated transformed ts-v-Src cells, measured by H_2DCFDA, were increased in a time- and concentration-dependent manner (Fig. 7A). Moreover, andrographolide treatment also increased the production of superoxide and reduced the intracellular level of glutathione in transformed ts-v-Src cells (Fig. 7B and C). In addition, the andrographolide-induced Hsp90 cleavage in ts-v-Src and Src531 cells was suppressed by the antioxidant N-acetylcysteine (NAC) (Fig. 7D). Furthermore, NAC treatment suppressed the andrographolide-mediated downregulation of v-Src and Src531 (Fig. 7D). Accordingly, pre-incubating ts-v-Src cells with NAC decreased andrographolide-induced apoptosis (Fig. 7E) and reversed the andrographolide-mediated inhibition of transformation (Fig. 7F). Similarly, the andrographolide-mediated Hsp90 cleavage, v-Src reduction and caspase-3 activation were also abolished by another antioxidant, Trolox (Fig. 7G). Together, these data suggested a critical role for ROS in andrographolide-mediated Hsp90 cleavage and the suppression of v-Src oncogenicity. The effects of andrographolide on Hsp90 were also examined in K562 cells, a human myelogenous leukemia line expressing the Hsp90 client protein Bcr-Abl. As shown in Fig. 8A, andrographolide treatment induced Hsp90 cleavage, Bcr-Abl degradation and caspase-3 activity in K562 cells and these effects were abolished by NAC pre-treatment (Fig. 8A). Furthermore, the activity of the andrographolide derivatives on Hsp90 cleavage correlated with the ability to downregulate Bcr-Abl and to induce apoptosis in K562 cells (Fig. 8B). Since andrographolide treatment exhibited consistent effects in both K562 and Src-transformed cells, it was concluded that andrographolide induced Hsp90 cleavage and destabilized Hsp90 client proteins in different types of cancer cells.

4. Discussion

We previously demonstrated that andrographolide impaired v-Src-mediated cell transformation by promoting v-Src degradation [36]. In this study, a strong correlation was observed between the

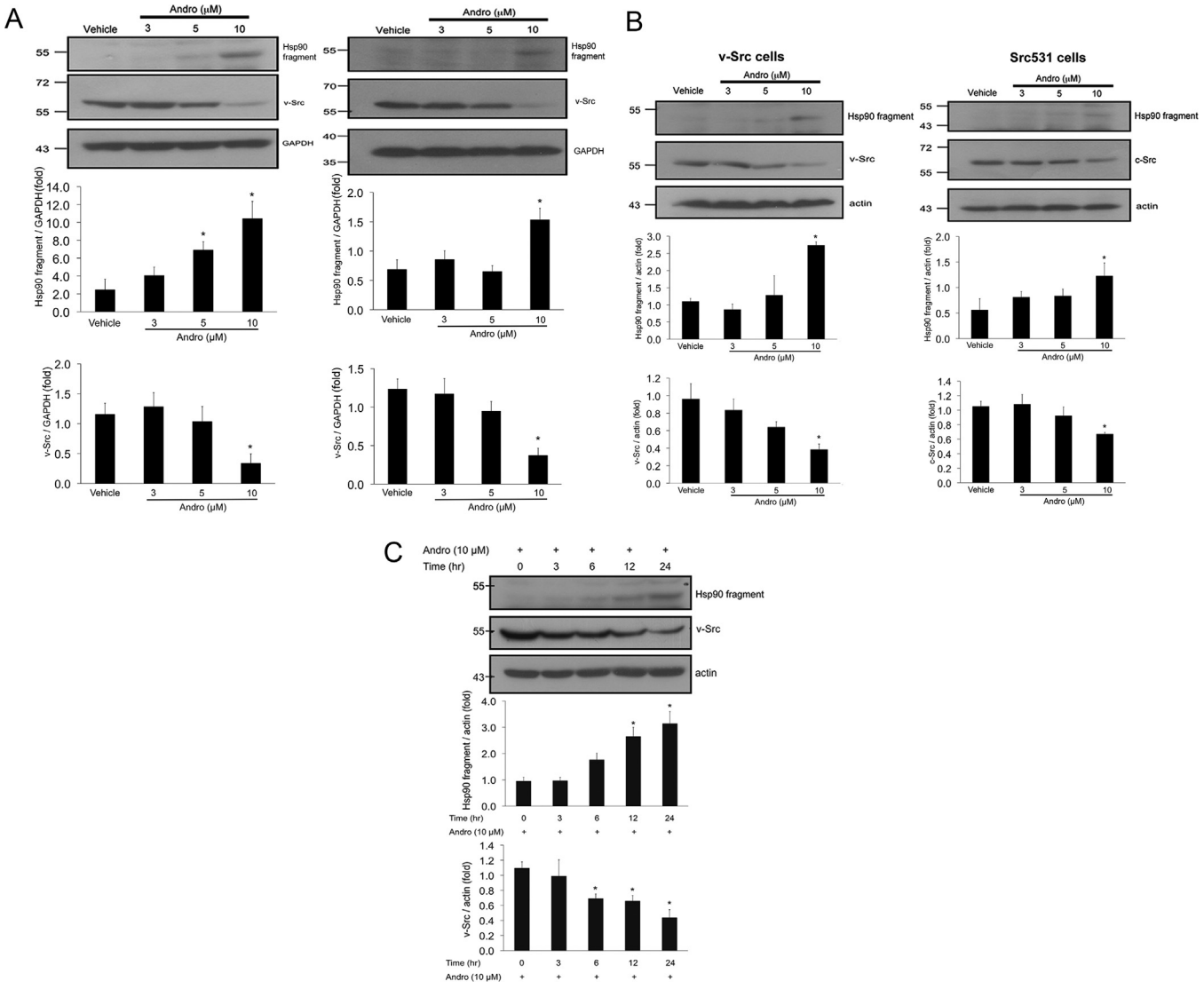

Fig. 4. The andrographolide-induced expression of the Hsp90 fragment was concentration- and time-dependent in Src-overexpressing cells. (A) *Left panel*: ts-v-Src cells grown at 39.5 °C were treated with different concentrations of andrographolide and incubated at 35 °C for 24 h. The expression of the Hsp90 fragment and v-Src was detected by Western blot. *Right panel*: ts-v-Src cells grown at 35 °C were treated with andrographolide, incubated for 24 h and analyzed by Western blot. (B) The v-Src- and Src531-overexpressing cells were treated with different concentrations of andrographolide, incubated for 24 h and analyzed by Western blot using antibodies against v-Src and c-Src respectively. (C) ts-v-Src cells grown at 35 °C were treated with andrographolide, incubated for different time periods and analyzed by Western blot. Actin was utilized as the internal control.

suppression of v-Src-mediated cell transformation and the downregulation of v-Src using andrographolide derivatives. Furthermore, using a proteomic approach, an Hsp90α fragment was identified that was specifically induced by andrographolide in v-Src-transformed cells (Fig. 3A and B). The production of this Hsp90 fragment, along with the downregulation of Src oncoprotein, was verified in cells transformed with either v-Src or a human truncated c-Src mutant (Src 531) and treated with andrographolide (Fig. 4). The andrographolide-induced Hsp90 fragment was enriched in detached apoptotic cells (Fig. 5). In addition, both andrographolide and its active derivatives induced Hsp90 cleavage, which was associated with cancer cell apoptosis (Fig. 6). Noticeably, ROS generated in response to andrographolide was required for Hsp90 cleavage, downregulating Src protein and suppressing the transformed phenotype and survival conferred by Src (Fig. 7). Importantly, ROS-dependent Hsp90 cleavage, the downregulation of Bcr-Abl (a hallmark Hsp90-client protein), and the induction of apoptosis were also observed in the human K562 leukemia cell line after treatment with andrographolide (Fig. 8). Together, our data demonstrated that andrographolide reduced the protein levels of v-Src and Bcr-Abl, which inhibited the cancer phenotypes and/or the survival of the cancer cells. Furthermore, andrographolide-mediated interference of "oncogene addiction" in cancer cells was related to the inhibition of Hsp90 function. Based on data from this study and a previous publication [36], a proposed model is described in Fig. 9.

In this study, we demonstrated that andrographolide-induced v-Src degradation was related to the inhibition of Hsp90 function, which supports the previous findings that Hsp90 chaperones are essential for Src stability and activity [13–15]. Notably, another Hsp90 client protein, Bcr-abl, was also downregulated by andrographolide (Fig. 8). A recent report demonstrated that andrographolide decreased the interaction of Hsp90 with the androgen receptor (AR), a client protein of Hsp90 [44]. Interestingly, andrographolide has been reported to elicit anticancer activities by reducing the protein levels of Akt, HIF-1α, and Cdk4 [45–47]. Because these proteins are all known Hsp90 clients, it is possible that andrographolide-mediated inhibition of Hsp90 is

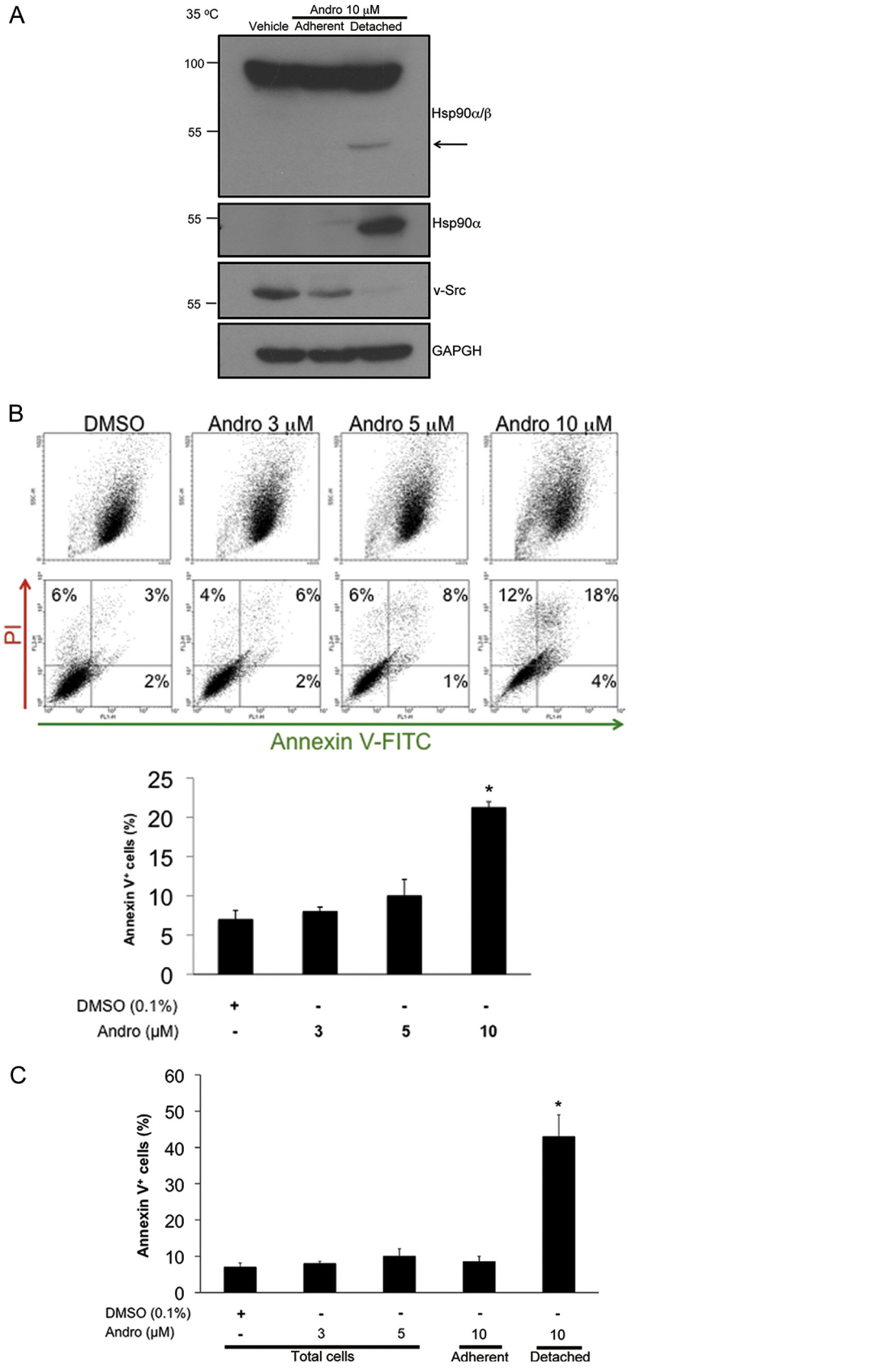

Fig. 5. Induction of the Hsp90 fragment correlated with the apoptosis of transformed ts-v-Src cells in response to andrographolide treatment. (A) The Hsp90α fragment was detected in transformed ts-v-Src cells (grown at 35 °C) after treatment with andrographolide (10 μM, 24 h). After drug treatment, both adherent and detached cells were collected and analyzed by Western blot using antibodies against Hsp90α/β, Hsp90α and v-Src. (B) Andrographolide-induced apoptosis in transformed ts-v-Src cells was measured using Annexin V/PI staining and flow cytometry (upper panel). The quantitative data on the apoptotic cells (Annexin V^+ cells) from three independent experiments are presented in the lower panel. (C) Andrographolide-induced apoptosis was greater in detached cells than in adherent cells. Data are presented as the mean ± S.E.M. Asterisk (*) indicates $p < 0.05$ versus vehicle control.

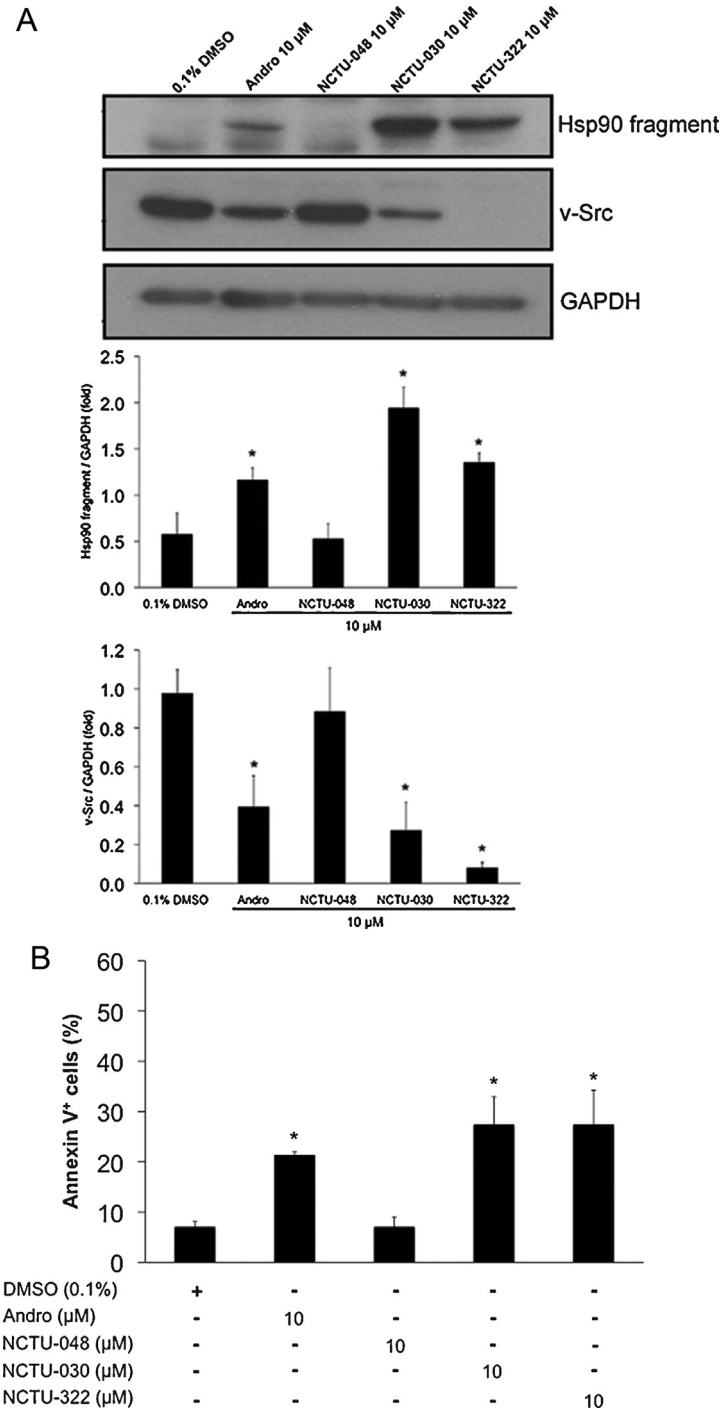

Fig. 6. The apoptosis-inducing activity of andrographolide and its derivatives correlated with the ability to induce Hsp90 cleavage. (A) The transformed ts-v-Src cells (grown at 35 °C) were treated with vehicle, andrographolide (Andro) or the derivatives for 24 h, then v-Src degradation and Hsp90 cleavage were measured by Western blot. GAPDH was utilized as an internal control. (B) The percentage of apoptotic cells after treatment with andrographolide or its analogues were measured by Annexin V/PI staining and flow cytometry. Data are presented as the mean ± S.E.M. Asterisk (*) indicates statistical significance versus vehicle control ($p < 0.05$).

involved in the downregulation of these proteins. Together, these data suggested that andrographolide decreased the stability of Hsp90 client proteins by inhibiting Hsp90 function.

The present study demonstrated that elevated ROS was associated with andrographolide-induced Hsp90 cleavage, oncoprotein degradation and cancer cell apoptosis (Fig. 7 and 8). In fact, andrographolide has been reported to induce ROS production under several circumstances [28,43]. Furthermore, several reports have demonstrated that oxidative stress induced by ascorbate/menadione [19], H_2O_2 [20,21] or arsenate [22] triggered Hsp90 cleavages, leading to the degradation of Hsp90 client proteins and cancer cell death [19,22]. Importantly, ROS-induced Hsp90 cleavage was observed in a large panel of cancer cell lines but not in non-transformed cells, indicating that Hsp90 cleavage is a specific event that occurs in cancer cells [19]. Taken together, these data suggested that ROS-dependent Hsp90 cleavage induced by andrographolide represents an effective mechanism to suppress cancer survival.

Several Hsp90 cleavage products have previously been identified in cancer cells under oxidative stress [19–22]. For example,

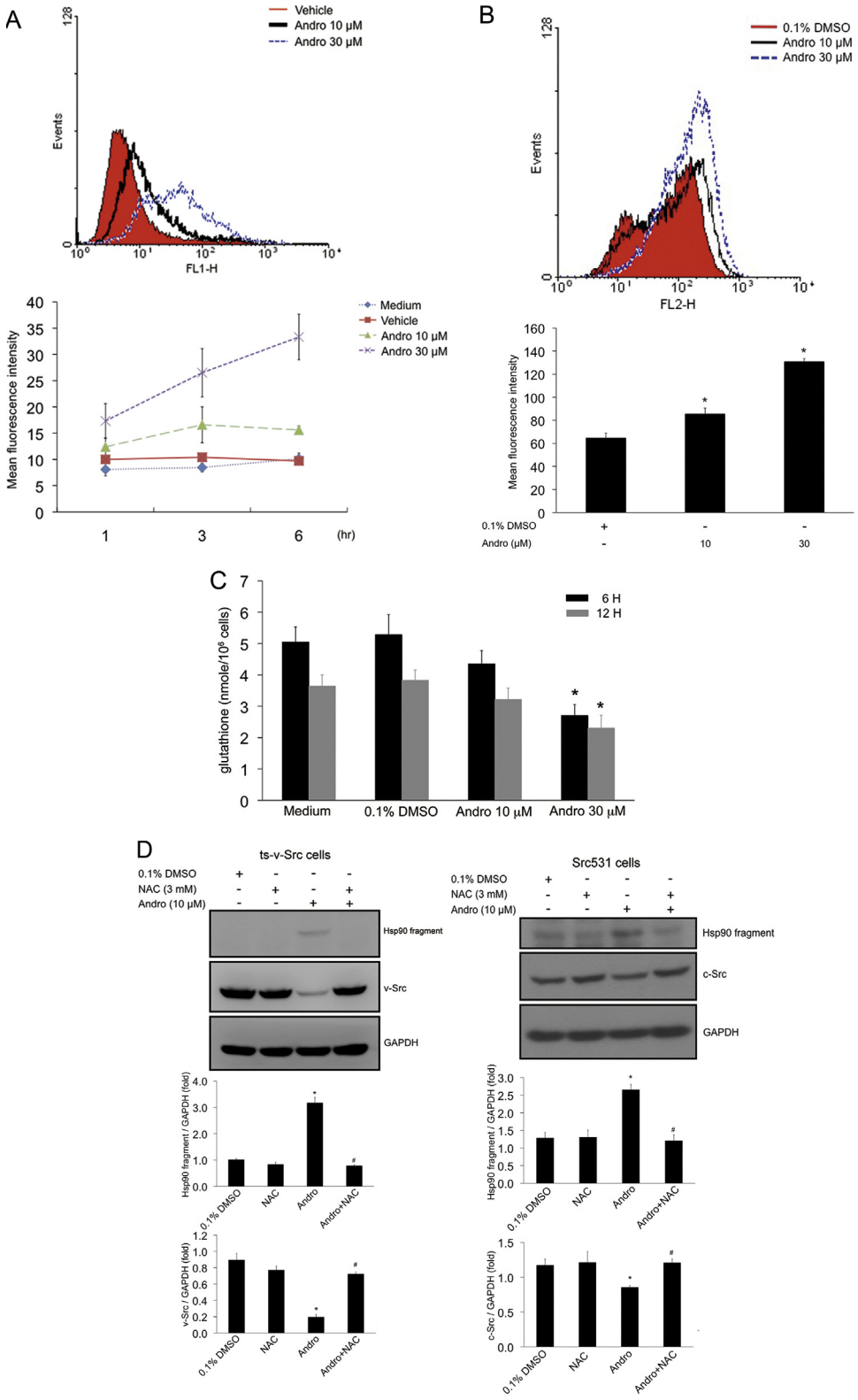

Fig. 7. Andrographolide-induced Hsp90 cleavage occurred via ROS production. (A) The intracellular ROS levels in transformed ts-v-Src cells treated with vehicle or andrographolide for 6 h were determined by H_2DCFDA treatment and flow cytometry. The mean fluorescence intensity of each sample was measured at the indicated time and concentration. (B) The superoxide levels in transformed ts-v-Src cells treated with vehicle or andrographolide (10 and 30 μM) for 12 h were detected using MitoSOX fluorescent dye and flow cytometry. The mean fluorescence intensity in each sample was shown. Data are presented as the mean ± S.E.M. from three independent experiments. Asterisk (*) indicates $p < 0.05$ versus vehicle control. (C) The glutathione content of andrographolide-treated cells at the indicated time and concentration was determined as described in Section 2. Data are presented as the mean ± S.E.M. from three independent experiments. Asterisk (*) indicates $p < 0.05$ versus vehicle control. (D) Transformed ts-v-Src or Src531#6 cells were incubated with or without N-acetylcysteine (NAC) for 1 h, exposed to andrographolide (10 μM for 24 h), and then analyzed for the expression of the Hsp90 fragment and Src protein by Western blot. (E) Transformed ts-v-Src cells (grown at 35 °C) were incubated with or without N-acetylcysteine (NAC) for 1 h, exposed to andrographolide (10 μM for 24 h), and then analyzed for the percentage of the apoptotic cells by Annexin V/PI staining and flow cytometry. Data are presented as the mean ± S.E.M. Asterisk (*) indicates statistical significance versus vehicle control ($p < 0.05$). (F) ts-v-Src cells grown at 39.5 °C were treated with or without NAC for 1 h, incubated with vehicle (0.1% DMSO) or andrographolide (5 μM), switched to 35 °C for 24 h, and then observed by microscopy for morphological alterations. (G) Transformed ts-v-Src cells (grown at 35 °C)

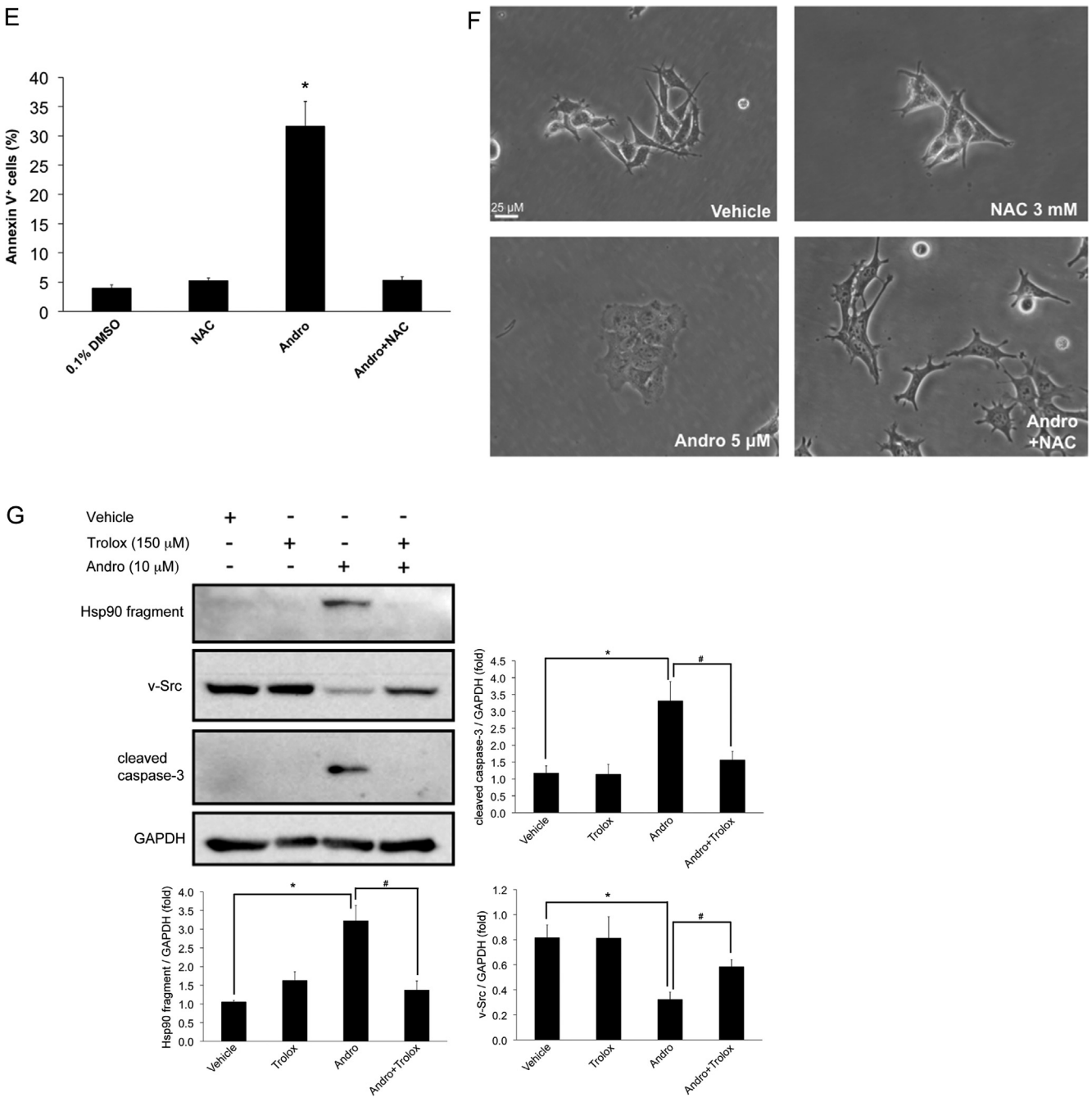

Fig. 7. (*Continued*).

UVB irradiation induced Hsp90β cleavage via caspase 10 in human A431 epidermoid carcinoma cells, resulting in the generation of a 55 kDa fragment near the N-terminus [48]. In addition, free radicals induced by ascorbate/menadione treatment initiated the cleavage of purified recombinant Hsp90 via a Fenton reaction in the presence of redox-active iron and ADP. This cleavage occurred in the conserved N-terminal regions of Hsp90α and Hsp90β and produced fragments of 72 and 18 kDa [42]. Moreover, an approximately 50 kDa cleavage fragment of Hsp90 was observed in H_2O_2-treated HeLa and HL-60 cells, but whether this cleavage fragment was from Hsp90α or Hsp90β has not been determined [20,21]. Based on our proteomics and Western blot data (Figs. 3B and 5A), the cleaved products (approximately 40 and 50 kDa) in this study were derived from Hsp90α. Hsp90 cleavage was therefore predicted to occur in the middle domain (amino acid 272–629), a region known to mediate the binding of client proteins and co-chaperones [1], and such cleavage presumably can diminish the chaperone function of Hsp90. We speculated that H_2O_2 is the primary mediator of andrographolide-induced Hsp90 cleavage because the cleavage products we observed were similar to those induced by H_2O_2 but not to those by ascorbate/menadione [20,21]. Furthermore, the direct treatment of Src-transformed cells

were incubated with or without Trolox (150 μM) for 1 h, exposed to andrographolide (10 μM for 24 h), and then analyzed for the expression of the Hsp90 fragment, v-Src, cleaved caspase-3 and GAPDH by Western blot. Data are presented as the mean ± S.E.M. Asterisk (*) and # respectively indicate statistical significance versus vehicle control or combined treatment ($p < 0.05$).

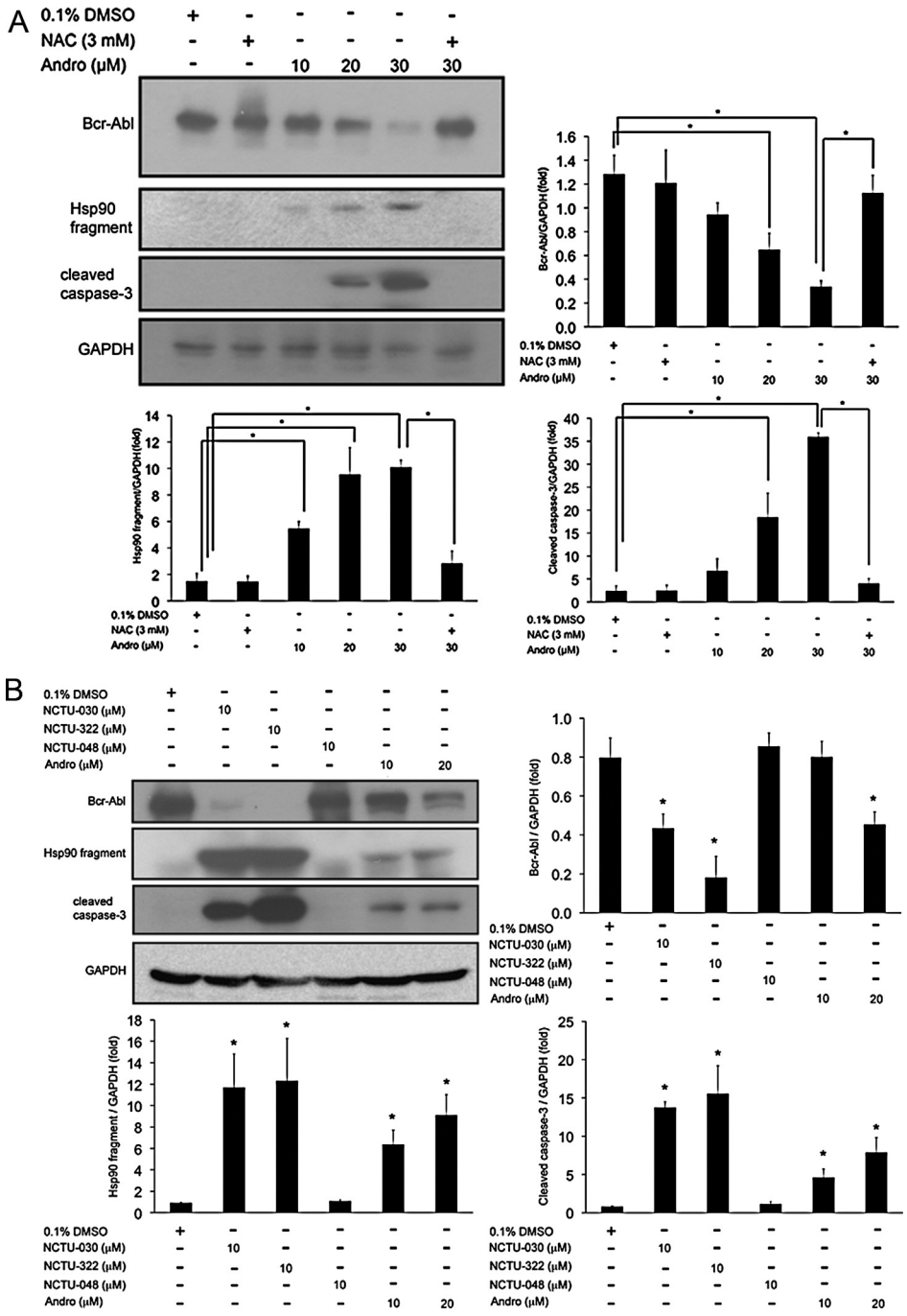

Fig. 8. Bcr-Abl downregulation and Hsp90 cleavage were induced by andrographolide in K562 cells via the ROS pathway. (A) Human K562 leukemia cells were incubated with or without NAC for 1 h, exposed to andrographolide (10, 20 or 30 μM for 24 h), and then analyzed by Western blot for the expression of Bcr-Abl, the Hsp90 fragment and cleaved caspase-3. (B) After treatment with vehicle, andrographolide (Andro) and the derivatives for 24 h, Bcr-Abl expression, Hsp90 cleavage and cleaved caspase-3 in K562 cells were measured by Western blot. GAPDH was utilized as an internal control. Data are presented as the mean ± S.E.M. from three independent experiments. Asterisk (*) indicates statistical significance versus vehicle or andrographolide-alone ($p < 0.05$).

with H_2O_2 produced a cleavage product of similar size to the 50 kDa fragment observed in this study (data not shown). It has been reported that Hsp90 is a substrate of granzyme B [49], but treatment with a granzyme B inhibitor did not block andrographolide-mediated Hsp90 cleavage (data not shown). Certainly, the exact cleavage site(s) in Hsp90 as well as the molecules involved in andrographolide-mediated Hsp90 cleavage merit additional investigation.

Hsp90 is considered to be a promising molecular target for cancer treatment [16]. Several Hsp90 inhibitors that are under clinical evaluation as anticancer agents primarily target the ATP-binding pocket in the N-terminus [16]. Among them, geldanamycin has been investigated the most in preclinical studies, but its therapeutic application is limited by significant hepatotoxicity [50]. 17-AAG, a geldanamycin derivative, is currently in a Phase III trial as a cancer therapeutic and has less toxicity, but has not been approved by the FDA. Furthermore, several traditional N-terminal Hsp90 inhibitors induce the expression of anti-apoptotic proteins, such as Hsp70 and Hsp27, which attenuate the anticancer effects of these inhibitors [51,52]. Therefore, the development of clinical Hsp90 inhibitors remains a challenge with a significant need. This study demonstrated that

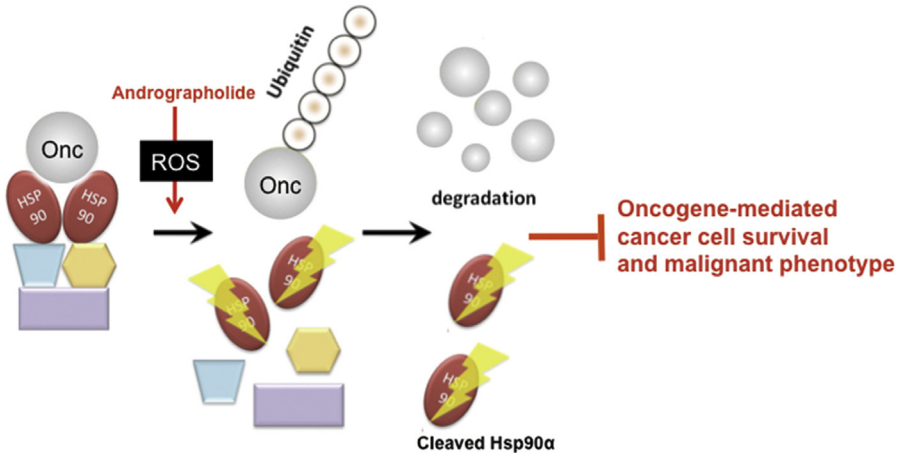

Fig. 9. A proposed model for andrographolide-mediated Hsp90 inhibition and oncogene degradation. Andrographolide-induced ROS triggers Hsp90 cleavage and affects the interaction between Hsp90 and its client proteins (such as v-Src and Bcr-Abl). The released client protein(s) are consequently degraded via the ubiquitin proteasome system, leading to the suppression of oncogene-elicited malignant phenotypes and cell survival.

andrographolide induced Hsp90 cleavage, which inhibited Hsp90 function via a different mechanism than the other small-molecule Hsp90 inhibitors. Notably, andrographolide-mediated Hsp90 cleavage did not increase the levels of anti-apoptotic Hsp70 (data not shown), which would be beneficial for cancer treatment. Another interesting phenomenon we observed was that andrographolide treatment led to the degradation of Bcr-Abl and apoptosis in K562 cells, a cell line derived from human chronic myelogenous leukemia (CML). Since the mechanism of action of current first-line drugs, such as Imatinib and Nilotinib, for clinical CML treatment involves inhibiting the kinase activity of Bcr-Abl [53], andrographolide-induced downregulation of Bcr-Abl at the protein level provides a novel strategy for CML treatment. Such an agent would be an ideal alternative for treating Imatinib-resistant CML.

Andrographolide and its source plant *Andrographis paniculata* exhibit anti-inflammatory activity [54], and both andrographolide alone and the plant extracts are commercially available worldwide as herbal supplements for treating upper respiratory diseases. *A. paniculata* extracts and andrographolide do not cause significant adverse side effects in patients, as determined in several clinical trials [55–58]. Recently, evidence of the anticancer activity of andrographolide has accumulated, and multiple molecular mechanisms and putative molecular targets have been proposed for its anticancer activity [54]. The current study demonstrated a novel anti-cancer mechanism of andrographolide that involved inhibiting Hsp90 function and downregulating Hsp90 client proteins, broadening the molecular basis of andrographolide-mediated anticancer effects.

Acknowledgements

This work was supported in part by grants from the National Science Council in Taiwan (NSC 99-2320-B-010-009-MY3), the Veterans General Hospital-Taipei, Taiwan (V101E5-005), Buddhist Dalin Tzu Chi General Hospital (DTCRD102-E-13) and the Ministry of Education, Aim for the Top University Plan (95A-C-D01-PPG-03).

References

[1] Whitesell L, Lindquist SL. HSP90 and the chaperoning of cancer. Nat Rev Cancer 2005;5:761–72.
[2] Conroy SE, Sasieni PD, Fentiman I, Latchman DS. Autoantibodies to the 90kDa heat shock protein and poor survival in breast cancer patients. Eur J Cancer 1998;34:942–3.
[3] Chant ID, Rose PE, Morris AG. Analysis of heat-shock protein expression in myeloid leukaemia cells by flow cytometry. Br J Haematol 1995;90:163–8.
[4] Yufu Y, Nishimura J, Nawata H. High constitutive expression of heat shock protein 90 alpha in human acute leukemia cells. Leuk Res 1992;16:597–605.
[5] Xu W, Neckers L. Targeting the molecular chaperone heat shock protein 90 provides a multifaceted effect on diverse cell signaling pathways of cancer cells. Clin Cancer Res 2007;13:1625–9.
[6] Hanahan D, Weinberg RA. The hallmarks of cancer. Cell 2000;100:57–70.
[7] Biamonte MA, Van de Water R, Arndt JW, Scannevin RH, Perret D, Lee WC. Heat shock protein 90: inhibitors in clinical trials. J Med Chem 2010;53:3–17.
[8] Bayraktar S, Rocha-Lima CM. Advanced or metastatic pancreatic cancer: molecular targeted therapies. Mt Sinai J Med 2010;77:606–19.
[9] Basso AD, Solit DB, Chiosis G, Giri B, Tsichlis P, Rosen N. Akt forms an intracellular complex with heat shock protein 90 (Hsp90) and Cdc37 and is destabilized by inhibitors of Hsp90 function. J Biol Chem 2002;277:39858–66.
[10] Jabbour E, Kantarjian H. Chronic myeloid leukemia: 2012 update on diagnosis, monitoring, and management. Am J Hematol 2012;87:1037–45.
[11] An WG, Schulte TW, Neckers LM. The heat shock protein 90 antagonist geldanamycin alters chaperone association with p210bcr-abl and v-src proteins before their degradation by the proteasome. Cell Growth Differ 2000;11:355–60.
[12] Gorre ME, Ellwood-Yen K, Chiosis G, Rosen N, Sawyers CL. BCR-ABL point mutants isolated from patients with imatinib mesylate-resistant chronic myeloid leukemia remain sensitive to inhibitors of the BCR-ABL chaperone heat shock protein 90. Blood 2002;100:3041–4.
[13] Xu Y, Singer MA, Lindquist S. Maturation of the tyrosine kinase c-src as a kinase and as a substrate depends on the molecular chaperone Hsp90. Proc Natl Acad Sci USA 1999;96:109–14.
[14] Whitesell L, Mimnaugh EG, De Costa B, Myers CE, Neckers LM. Inhibition of heat shock protein HSP90-pp60v-src heteroprotein complex formation by benzoquinone ansamycins: essential role for stress proteins in oncogenic transformation. Proc Natl Acad Sci USA 1994;91:8324–8.
[15] Xu Y, Lindquist S. Heat-shock protein hsp90 governs the activity of pp60v-src kinase. Proc Natl Acad Sci USA 1993;90:7074–8.
[16] Trepel J, Mollapour M, Giaccone G, Neckers L. Targeting the dynamic HSP90 complex in cancer. Nat Rev Cancer 2010;10:537–49.
[17] Meyer P, Prodromou C, Hu B, Vaughan C, Roe SM, Panaretou B, et al. Structural and functional analysis of the middle segment of hsp90: implications for ATP hydrolysis and client protein and cochaperone interactions. Mol Cell 2003;11:647–58.
[18] Petrikaite V, Matulis D. Binding of natural and synthetic inhibitors to human heat shock protein 90 and their clinical application. Medicina (Kaunas) 2011;47:413–20.
[19] Beck R, Verrax J, Gonze T, Zappone M, Pedrosa RC, Taper H, et al. Hsp90 cleavage by an oxidative stress leads to its client proteins degradation and cancer cell death. Biochem Pharmacol 2009;77:375–83.
[20] Panopoulos A, Harraz M, Engelhardt JF, Zandi E. Iron-mediated H_2O_2 production as a mechanism for cell type-specific inhibition of tumor necrosis factor alpha-induced but not interleukin-1beta-induced IkappaB kinase complex/nuclear factor-kappaB activation. J Biol Chem 2005;280:2912–23.
[21] Pantano C, Shrivastava P, McElhinney B, Janssen-Heininger Y. Hydrogen peroxide signaling through tumor necrosis factor receptor 1 leads to selective activation of c-Jun N-terminal kinase. J Biol Chem 2003;278:44091–96.
[22] Shen SC, Yang LY, Lin HY, Wu CY, Su TH, Chen YC. Reactive oxygen species-dependent HSP90 protein cleavage participates in arsenical As(+3)- and MMA(+3)-induced apoptosis through inhibition of telomerase activity via JNK activation. Toxicol Appl Pharmacol 2008;229:239–51.

[23] Abu-Ghefreh AA, Canatan H, Ezeamuzie CI. In vitro and in vivo anti-inflammatory effects of andrographolide. Int Immunopharmacol 2009;9:313–8.
[24] Chandrasekaran CV, Thiyagarajan P, Deepak HB, Agarwal A. In vitro modulation of LPS/calcimycin induced inflammatory and allergic mediators by pure compounds of Andrographis paniculata (King of bitters) extract. Int Immunopharmacol 2011;11:79–84.
[25] Lee KC, Chang HH, Chung YH, Lee TY. Andrographolide acts as an anti-inflammatory agent in LPS-stimulated RAW264.7 macrophages by inhibiting STAT3-mediated suppression of the NF-kappaB pathway. J Ethnopharmacol 2011;135:678–84.
[26] Bao Z, Guan S, Cheng C, Wu S, Wong SH, Kemeny DM, et al. A novel antiinflammatory role for andrographolide in asthma via inhibition of the nuclear factor-kappaB pathway. Am J Respir Crit Care Med 2009;179:657–65.
[27] Shi MD, Lin HH, Lee YC, Chao JK, Lin RA, Chen JH. Inhibition of cell-cycle progression in human colorectal carcinoma Lovo cells by andrographolide. Chem Biol Interact 2008;174:201–10.
[28] Li J, Cheung HY, Zhang Z, Chan GK, Fong WF. Andrographolide induces cell cycle arrest at G2/M phase and cell death in HepG2 cells via alteration of reactive oxygen species. Eur J Pharmacol 2007;568:31–44.
[29] Zhou J, Zhang S, Ong CN, Shen HM. Critical role of pro-apoptotic Bcl-2 family members in andrographolide-induced apoptosis in human cancer cells. Biochem Pharmacol 2006;72:132–44.
[30] Zhou J, Lu GD, Ong CS, Ong CN, Shen HM. Andrographolide sensitizes cancer cells to TRAIL-induced apoptosis via p53-mediated death receptor 4 up-regulation. Mol Cancer Ther 2008;7:2170–80.
[31] Chen W, Feng L, Nie H, Zheng X. Andrographolide induces autophagic cell death in human liver cancer cells through cyclophilin D-mediated mitochondrial permeability transition pore. Carcinogenesis 2012.
[32] Hung SK, Hung LC, Kuo CD, Lee KY, Lee MS, Lin HY, et al. Andrographolide sensitizes Ras-transformed cells to radiation in vitro and in vivo. Int J Radiat Oncol Biol Phys 2010;77:1232–9.
[33] Zhou J, Hu SE, Tan SH, Cao R, Chen Y, Xia D, et al. Andrographolide sensitizes cisplatin-induced apoptosis via suppression of autophagosome-lysosome fusion in human cancer cells. Autophagy 2012;8:338–49.
[34] Shi MD, Lin HH, Chiang TA, Tsai LY, Tsai SM, Lee YC, et al. Andrographolide could inhibit human colorectal carcinoma Lovo cells migration and invasion via down-regulation of MMP-7 expression. Chem Biol Interact 2009;180:344–52.
[35] Chao HP, Kuo CD, Chiu JH, Fu SL. Andrographolide exhibits anti-invasive activity against colon cancer cells via inhibition of MMP2 activity. Planta Med 2010;76:1827–33.
[36] Liang FP, Lin CH, Kuo CD, Chao HP, Fu SL. Suppression of v-Src transformation by andrographolide via degradation of the v-Src protein and attenuation of the Erk signaling pathway. J Biol Chem 2008;283:5023–33.
[37] Irby RB, Mao W, Coppola D, Kang J, Loubeau JM, Trudeau W, et al. Activating SRC mutation in a subset of advanced human colon cancers. Nat Genet 1999;21:187–90.
[38] Hung LC, Lin CC, Hung SK, Wu BC, Jan MD, Liou SH, et al. A synthetic analog of alpha-galactosylceramide induces macrophage activation via the TLR4-signaling pathways. Biochem Pharmacol 2007;73:1957–70.
[39] Chiou YY, Fu SL, Lin WJ, Lin CH. Proteomics analysis of in vitro protein methylation during Src-induced transformation. Electrophoresis 2012;33:451–61.
[40] Huang YL, Chung TW, Chang CM, Chen CH, Liao CC, Tsay YG, et al. Qualitative analysis of the fluorophosphonate-based chemical probes using the serine hydrolases from mouse liver and poly-3-hydroxybutyrate depolymerase (PhaZ) from Bacillus thuringiensis. Anal Bioanal Chem 2012;404:2387–96.
[41] Soga S, Shiotsu Y, Akinaga S, Sharma SV. Development of radicicol analogues. Curr Cancer Drug Targets 2003;3:359–69.
[42] Beck R, Dejeans N, Glorieux C, Creton M, Delaive E, Dieu M, et al. Hsp90 is cleaved by reactive oxygen species at a highly conserved N-terminal amino acid motif. PLoS One 2012;7:e40795.
[43] Yang S, Evens AM, Prachand S, Singh AT, Bhalla S, David K, et al. Mitochondrial-mediated apoptosis in lymphoma cells by the diterpenoid lactone andrographolide, the active component of Andrographis paniculata. Clin Cancer Res 2010;16:4755–68.
[44] Liu C, Nadiminty N, Tummala R, Chun JY, Lou W, Zhu Y, et al. Andrographolide targets androgen receptor pathway in castration-resistant prostate cancer. Genes Cancer 2011;2:151–9.
[45] Li Y, Zhang P, Qiu F, Chen L, Miao C, Li J, et al. Inactivation of PI3K/Akt signaling mediates proliferation inhibition and G2/M phase arrest induced by andrographolide in human glioblastoma cells. Life Sci 2012;90:962–7.
[46] Lee YC, Lin HH, Hsu CH, Wang CJ, Chiang TA, Chen JH. Inhibitory effects of andrographolide on migration and invasion in human non-small cell lung cancer A549 cells via down-regulation of PI3K/Akt signaling pathway. Eur J Pharmacol 2010;632:23–32.
[47] Lin HH, Tsai CW, Chou FP, Wang CJ, Hsuan SW, Wang CK, et al. Andrographolide down-regulates hypoxia-inducible factor-1alpha in human non-small cell lung cancer A549 cells. Toxicol Appl Pharmacol 2011;250:336–45.
[48] Chen H, Xia Y, Fang D, Hawke D, Lu Z. Caspase-10-mediated heat shock protein 90 beta cleavage promotes UVB irradiation-induced cell apoptosis. Mol Cell Biol 2009;29:3657–64.
[49] Hostetter DR, Loeb CR, Chu F, Craik CS. Hip is a pro-survival substrate of granzyme B. J Biol Chem 2007;282:27865–74.
[50] Supko JG, Hickman RL, Grever MR, Malspeis L. Preclinical pharmacologic evaluation of geldanamycin as an antitumor agent. Cancer Chemother Pharmacol 1995;36:305–15.
[51] Beck R, Dejeans N, Glorieux C, Pedrosa RC, Vasquez D, Valderrama JA, et al. Molecular chaperone Hsp90 as a target for oxidant-based anticancer therapies. Curr Med Chem 2011;18:2816–25.
[52] McCollum AK, Teneyck CJ, Sauer BM, Toft DO, Erlichman C. Up-regulation of heat shock protein 27 induces resistance to 17-allylamino-demethoxygeldanamycin through a glutathione-mediated mechanism. Cancer Res 2006;66:10967–75.
[53] Druker BJ, Tamura S, Buchdunger E, Ohno S, Segal GM, Fanning S, et al. Effects of a selective inhibitor of the Abl tyrosine kinase on the growth of Bcr-Abl positive cells. Nat Med 1996;2:561–6.
[54] Lim JC, Chan TK, Ng DS, Sagineedu SR, Stanslas J, Wong WS. Andrographolide and its analogues: versatile bioactive molecules for combating inflammation and cancer. Clin Exp Pharmacol Physiol 2012;39:300–10.
[55] Poolsup N, Suthisisang C, Prathanturarug S, Asawamekin A, Chanchareon U. Andrographis paniculata in the symptomatic treatment of uncomplicated upper respiratory tract infection: systematic review of randomized controlled trials. J Clin Pharm Ther 2004;29:37–45.
[56] He Q, Dong J, Zhen H, Ying Y, Zhang J, Li Q, et al. A small molecule significantly inhibits the bcr/abl fusion gene at the mRNA level in human chronic myelogenous leukemia. Leuk Res 2011;35:1074–9.
[57] Chang J, Zhang RM, Zhang Y, Chen ZB, Zhang ZM, Xu Q, et al. Andrographolide drop-pill in treatment of acute upper respiratory tract infection with external wind-heat syndrome: a multicenter and randomized controlled trial. Zhong Xi Yi Jie He Xue Bao 2008;6:1238–45.
[58] Burgos RA, Hancke JL, Bertoglio JC, Aguirre V, Arriagada S, Calvo M, et al. Efficacy of an Andrographis paniculata composition for the relief of rheumatoid arthritis symptoms: a prospective randomized placebo-controlled trial. Clin Rheumatol 2009;28:931–46.